



Chiang Mai J. Sci. 2019; 46(1) : 93-105

<http://it.science.cmu.ac.th/ejournal/>

Contributed Paper

Predicting the Binding Affinity of P38 Map Kinase Inhibitors using Free Energy Calculations

Warabhorn Boonyarat [a,b], Patchreenart Saparpakorn [a,b] and Supa Hannongbua* [a,b]

[a] Department of Chemistry, Faculty of Science, Kasetsart University, Bangkok 10900, Thailand.

[b] Center for Advanced Studies in Nanotechnology and Its Applications in Chemical,

Food and Agricultural Industries, KU institute for Advanced Studies, Kasetsart University,

Bangkok 10900, Thailand.

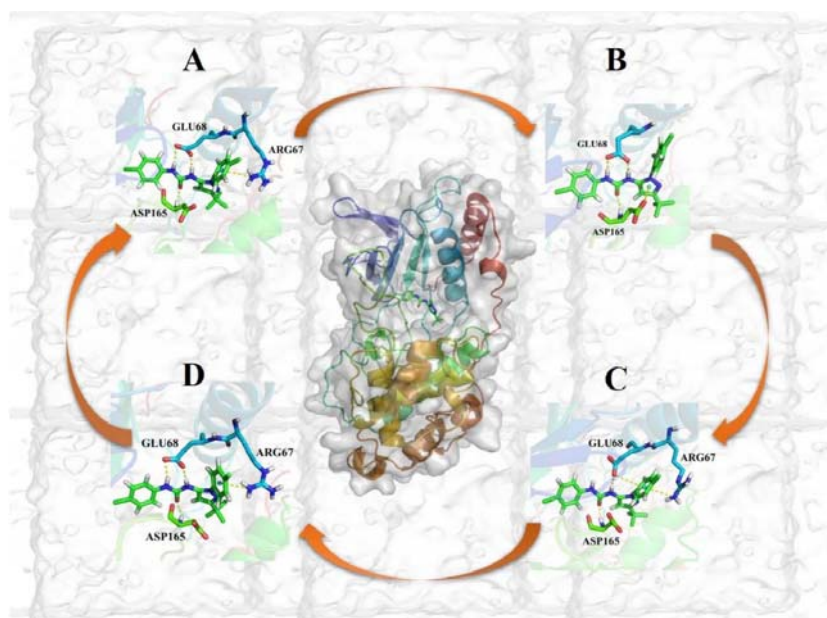
*Author for correspondence; e-mail: fscisph@ku.ac.th

Received: 21 July 2018

Accepted: 4 August 2018

Graphical Abstract

The cycle of thermodynamic integration (TI) free energy profiles indicate the interactions of type II inhibitor inside the p38 MAP kinase protein. Orientation and molecular flexibility of inhibitor depended on hydrogen bonds and pi-stacking interactions with Arg67, Glu68, and Asp165 of kinase protein.



ABSTRACT

The major challenge of drug design efforts is focused on inhibitors of p38 MAP kinase (MAPK14) proteins to develop the drug resistance caused by spontaneous mutations in the kinase domain. Despite the central role in structure-based drug design of kinase in order to determine the position, orientation and conformation of small inhibitors in protein, we investigated how DFG (Asp-Phe-Gly)-in and DFG-out active sites are important in type I inhibitor binding to ATP site of kinase. The investigation has been focused on the key interaction as hydrogen bond and pi-stacking, based on molecular dynamics (MD) simulations. Moreover, the thermodynamic integration (TI) free energy calculations has been used to identify the type II inhibitors which are stable binding to the allosteric site of p38 MAP kinase. Diaryl urea of type II inhibitor showed to be involved in an extensive hydrogen bond network and proved critical for binding activity. TI free energy calculations are in agreement with the experiment. The results confirmed that interaction with type II inhibitors is compatible with DFG-out conformation of p38 MAP kinase. Therefore, the MD simulations can successfully predict the interaction of inhibitors in P38 MAP kinase and determine the differences in binding affinity which can be helpful to develop new type II inhibitors for the treatment of many diseases.

Keywords: P38 MAP kinase, thermodynamic integration free energy, molecular dynamics simulations, drug design, protein-inhibitor interactions

1. INTRODUCTION

Kinases are involved in a wide range of disease conditions from inflammation to oncogenesis and as such are increasingly viewed as major targets for therapeutic intervention. Different protein kinases recognize a narrow range of substrates which is a factor that can be exploited pharmaceutically to create specificity. P38 mitogen-activated protein (MAP) kinases pathway plays an important role in inflammation and physiological processes that there are effective to the regulation of stress response pathways [1] such as cytokines, ultraviolet irradiation, heat shock, and osmotic stress, arsenite [2-4], and are also involved in cell differentiation, apoptosis, and autophagy. Furthermore, this pathway controls the production and secretion of pro-inflammatory cytokines such as tumor necrosis factor- α (TNF α), interleukin-6 (IL-6) and interleukin-1 α (IL-1 β) [5]. The major of p38 MAP kinase has been a

target for anti-inflammatory therapy [6] and important targets for drug discovery.

P38 MAPK kinases have been studied in decades, therefore, the p38 proteins have renewed their fames in the recent drug development arena [7] since novel targets and functions have been recently identified via protein-protein interaction (PPI). There are four isoforms for p38 MAP kinases, namely, MAPK11/12/13 and 14. In this work, we are focusing on p38-alpha MAPK14 due to being an enzyme in the human disease and known as stress-activated protein kinase. The structure of protein kinase consists of two major subdomains which are the N-terminal and C-terminal lobes [8]. The active loop belongs to the C-terminal lobe and closes to the hinge region controls the conformational transition between the active conformation and the inactive conformation of the kinase [9]. A type of kinase inhibitors are ATP-competitive

molecules, which form hydrogen bonds at the hinge region (ATP binding site) of the active Asp-Phe-Gly (DFG)-in kinase conformation. The ATP binding site is well-known for the selective binding site for type I inhibitors [10]. However, the crystal structures of kinase have shown that kinase inhibitors occupy both the ATP-binding pocket and the allosteric pocket [11]. The kinase activation can also be blocked by the type II inhibitors, which bind to the inactive (DFG-out) conformations of the kinase. The type-I and type-II inhibitors bind to binding sites with different conformations of the DFG in kinases [12].

P38 MAP kinases are characterized by the DFG-loop conformation which is typically found in the active, or DFG-in

conformation. The DFG-loop transition is triggered by the shift of the Phe169 side chain by 10 Å and 180° flip from DFG-in conformation to DFG-out conformation [13]. The DFG-in conformation accesses to the deep pocket in hindered by Phe169 [14], whereas in the DFG-out conformation, Phe169 locates nearby α -C helix in the ATP binding pocket [15]. Therefore, analysis of kinase structures is of outstanding interest to the structure between the active and inactive kinase conformations. These inhibitors are found to be the keys of therapeutic strategy for the treatment of a diverse range of pathological [16]. The conformations of DFG-in and DFG-out are shown in Figure 1.

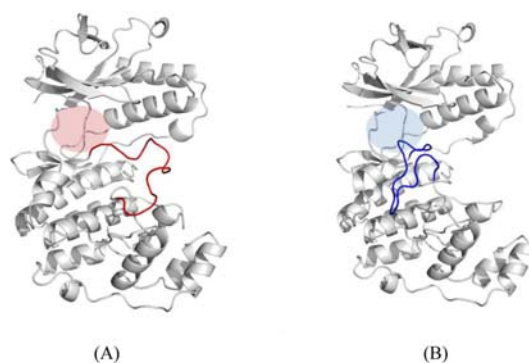


Figure 1. Structures of (A) DFG motif in and (B) out conformations of p38 MAP kinase.

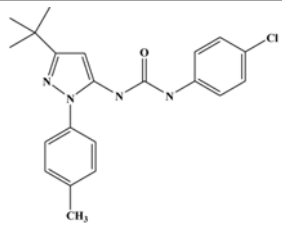
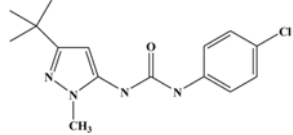
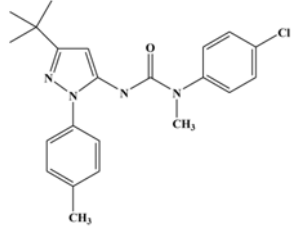
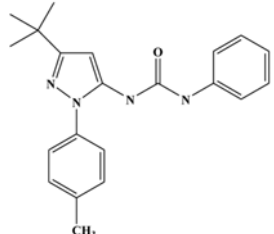
Considering the nature of the amino acids in the ATP pocket, one would expect the methods for discriminating between DFG-in and DFG-out binders to guide for innovative compound design. The importance of these three amino acids (DFG) in the binding is also interesting. From the crystal structures of SB-203580 inhibitor complexed with the p38 MAP kinase, both DFG-in, mutation of active conformation (GFG-in, DGG-in), and DFG-out conformations of the kinase are found. Therefore, in order to investigate the effect of the binding interaction

in both conformations, the interaction between the p38 MAP kinase and SB-203580 inhibitor which binds in the ATP-binding pocket are studied using MD simulations. [17]

In the case of the DFG-out conformation, a set of the type II inhibitors (Inhibitors A-D) are selected for the study and the experimental thermodynamic data of these inhibitors are shown in Table 1. The effect of the substituent of type II inhibitor in the DFG-out conformations is investigated by thermodynamics integration free energy calculations. The insight information for

the binding of inhibitors in DFG-in and DFG-out conformations will be helpful to explain the inhibition of the p38 MAP kinase inhibitors.

Table 1. Chemical structures and experimental K_D and ΔG for the selected p38 MAP kinase inhibitors.

Inhibitor	Structure	K_D (nM)	ΔG (kJ/mol)
A		8	-46.21
B		1160	-33.86
C		7500	-29.25
D		21	-43.82

* Data for compounds 1, 2, 3 and 4 (K_D) at 296 K were taken from Refs [21, 35].

2. METHODS

2.1 Molecular Dynamics (MD)

Simulations

All simulations are performed using the GROMACS 3.3.3 [18] simulation package in conjunction with the GROMOS 54A7 [19] force field. For the study of Type I inhibitor, all available initial structures of p38 MAP kinase (379 residues) complexed with SB203580 (Pyridinyl imidazole (4-[5-(4-fluoro-phenyl)-2-(4-methanesulfinyl-phenyl)-3H-imidazole-4-yl]-pyridine])

are taken from the PDB entries 1A9U (DFG-in), 2EWA(GFG-in), 3GCP(DGG-in), 3MPA(DFG-out), 3OBG(DFG-out) and 3ZS5 (DFG-out), respectively [17, 20-22]. The substructure of SB203580 can be decomposed into five principal moieties: (I) imidazole, (II) fluorobenzene, (III) pyridine, (IV) benzene, and (V) sulfoxide. For the study of Type II inhibitor, the initial structure of p38 MAP kinase (360 residues) complexed with inhibitor B, BMU (1-(5-tert-butyl-2-methyl-2h-pyrazol-3-yl)-3-(4-chloro-phenyl)-

urea) is taken from the PDB entry 1KV1. The structures of inhibitors A, C, and D are constructed based in the structure of inhibitor B. The topologies of all inhibitors are generated using the ‘automated topology builder’ (ATB, <http://compmio.biosci.uq.edu.au/atb/>) and optimized manually [23].

Each complex is placed in a dodecahedral periodic box and solvated with simple point charge (SPC) water molecules [24]. The protonation state of titratable groups is chosen appropriately to pH 7.0 giving a total charge on the system of -8 e. Each complex is energy minimized and the system equilibrated for 200 ps with the heavy atoms of the protein positionally restrained before commencing a series of unrestrained molecular dynamics (MD) simulations. All simulations are performed at constant temperature (298 K) and pressure (1 atm) using a Berendsen thermostat (coupling time of 0.1 ps) and barostat (coupling time of 1.0 ps and isothermal compressibility of 4.575×10^{-4} (kJ/mol/nm³)⁻¹) [25]. A triple-range cutoff is used. Interactions within a shorter-range cutoff of 0.8 nm are updated every step (0.002 ps). Interactions within the longer-range cutoff of 1.4 nm are updated 0.010 ps together with the pair list. To correct for the truncation of the electrostatic interactions beyond the 1.4 nm long-range cutoff a reaction-field correction is applied using a dielectric permittivity of 78. The equations of motion are integrated using the leapfrog scheme. Initial velocities at a given temperature are taken from a Maxwell-Boltzmann distribution. All bonds are constrained using the SHAKE algorithm with a geometric tolerance of 0.0001 [26].

2.2 Free Energy Calculations

The difference Gibbs free energy between alternate orientation and

conformations of the inhibitors is estimated using the coupling parameter (λ) approach in conjunction with the thermodynamic integration (TI) formula [27].

$$\Delta G = \int_{\lambda=0}^{\lambda=1} \left\langle \frac{\partial H}{\partial \lambda} \right\rangle_{\lambda} d\lambda \quad (1)$$

Where $\lambda = 0$ corresponded to the initial state of the system and $\lambda = 1$ corresponding to the final state of the system. H is the Hamiltonian of the system and the brackets $\langle \dots \rangle_{\lambda}$ correspond to an average over an equilibrium ensemble at λ . The relative free energy of binding $\Delta\Delta G$ is determined from the difference in the change in free energy of performing the same mutation-free in solution and bound to the protein. To change the conformation of the molecule alchemical mutations are performed in which the orientation of the group is restrained, and the interactions of the group with the environment in one orientation are decreased from 1 to 0 while in another orientation it is increased from 0 to 1. The free energies are then corrected for the effect of the restraining potential by estimating the work required to impose the restraint in water. Equation one is integrated by performing separate simulations at a series of 21 (0.00, 0.01, 0.02 ... 0.05, 0.10, 0.20, 0.90, 0.95, 0.96, ..., 1.00) λ points in both the bound and unbound states. The systems are first equilibrated for 200 ps followed by production runs of 1 ns to estimate $dH/d\lambda$ obtained at each λ . To prevent numerical instabilities as atoms are created or destroyed the soft-core potential as described by Beutler *et. al.* is used [28, 29] with $\alpha_{ij}^{1,1} = \alpha_{ij}^c = 0.5$ nm². The area beneath the curve in 1 is estimated using a trapezoidal approximation. The statistical error at each λ -point is estimated using a block averaging technique [30].

3. RESULTS AND DISCUSSION

3.1 Validation of p38 MAP Kinase Bound to SB-203580

The crystal structures of the type I inhibitor (SB-203580) in complexed with the DFG-in, GFG-in, DGG-in, and DFG-out conformations p38 MAP kinases [17] reveal the similar binding orientation of SB-203580. To explore the dynamic stability of complexes and explain the SB-203580 binding orientation, MD simulations for 10 ns are applied and the RMSD of protein and active site amino acids reveal the stabilization of the system as shown in Figure 2. The fluctuations are less about 1 Å. In the case of -in conformations as shown in Figures 2A-C, the RMSD values of the DFG-in, GFG-in, DGG-in show less fluctuation than those of DFG-out conformations. In the ATP active site, the type I inhibitor forms two hydrogen bonds with the backbone that are NH of Met106 and O of His104 in the hinge region and the NH of Asp165 of the DFG-in loop movement [31]. The Phe166 structure is flipping out in the DFG loop [32], which is formed with SB-203580 by the pi-pi stacking [33, 34]. These information indicates the stabilized interaction of -in conformation.

The RMSD values of SB-203580 in three DFG-out conformations show the higher fluctuations and the sharp change of the RMSD than those of DFG-in and mutated DFG-in indicating that the type I inhibitor (SB-203580) has a stable binding with DFG-in and DFG-in mutate P38 MAP kinase and less stable in DFG-out MAP kinase.

Analyses of root-mean-square fluctuation (RMSF) versus the residue number for complexes are shown in Figure 3. The high RMSF values are found for the residues within in the flexible loops. The observations are in agreement with the experimental results from x-ray crystallographic data. The fluctuation of the active site for type I inhibitor is significant and the high fluctuation is found relatively to the ATP active site region (residues 32, 50, 104, 106, 151, and 165-167). The RMSF values of DFG-out conformation are higher than those in DFG-in and mutated DFG-in indicating the less stable interaction to the inhibitor.

3.2 Conformation of the ATP Active Site Region

The snapshot at 0, 5, and 10 ns of six complexes are shown in Figure 4. To further investigation on inhibitors-p38 MAP kinase interactions in the binding site, the snapshots are taken from the 10 ns MD trajectory. The hydrogen bonds and stacking interaction with the key residues in the binding pocket are shown in Figure 5. It can be seen that the NH of Met106 formed a hydrogen bond with N atom of imidazole of inhibitors in all systems. The DFG-in (1A9U) and mutant (3MPA and 3OBG) proteins form hydrogen bonds between SB-203580 and Gly33, Lys50, and Ser151. In the case of DFG-out, structure of 3GCP, 3ZS5, and 2EWA complexes form less hydrogen bond and pi-stacking networks to Lys50, Tyr32, and Phe166 (Figures 5D-F).

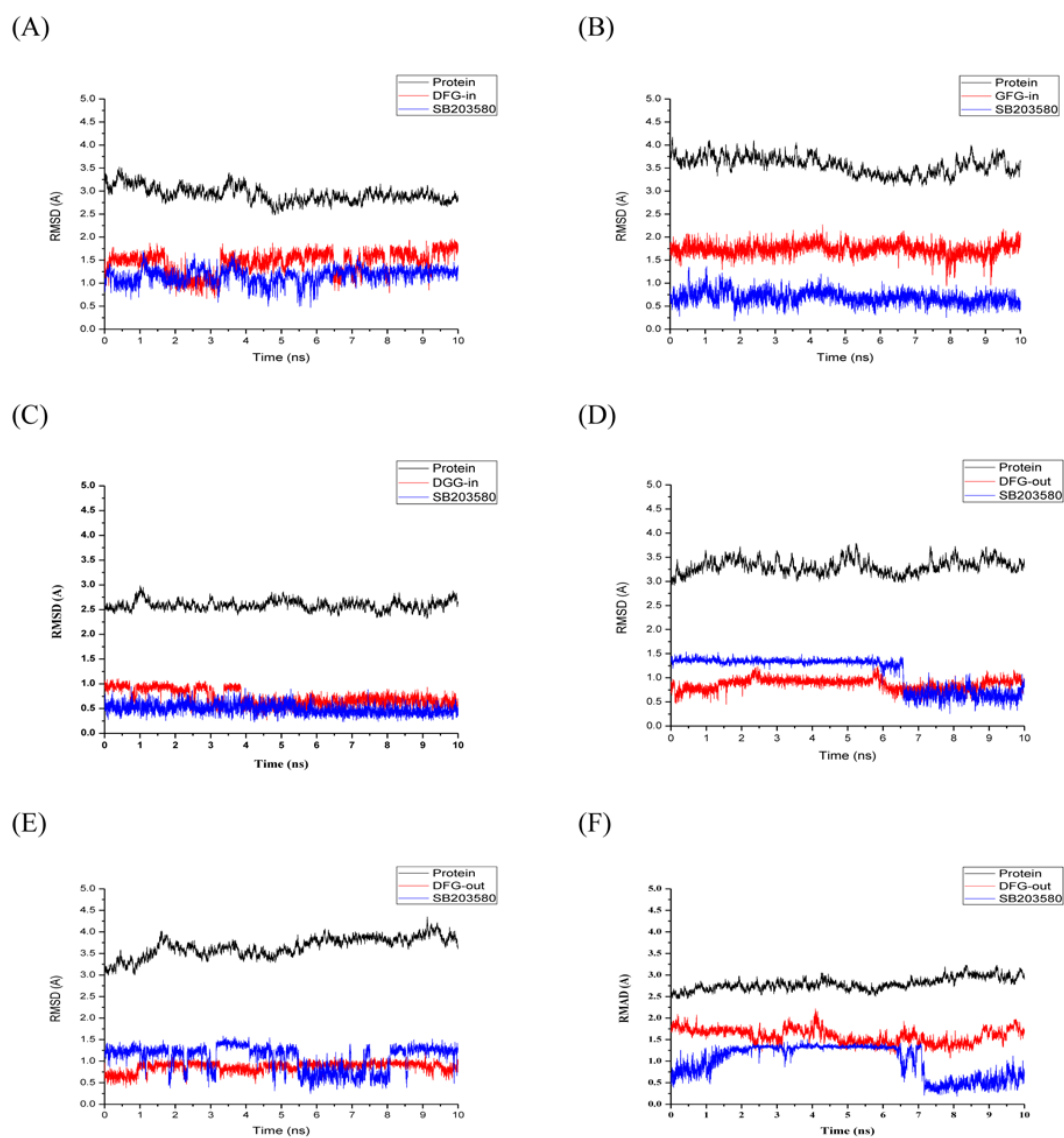


Figure 2. RMSDs of the protein, DFG, and SB-203580 for pdb entries (A) 1A9U, (B) 3MPA, (C) 3OBG, (D) 3GCP, (E) 3ZS5 and (F) 2EWA bound to SB203580 as a function of simulation time.

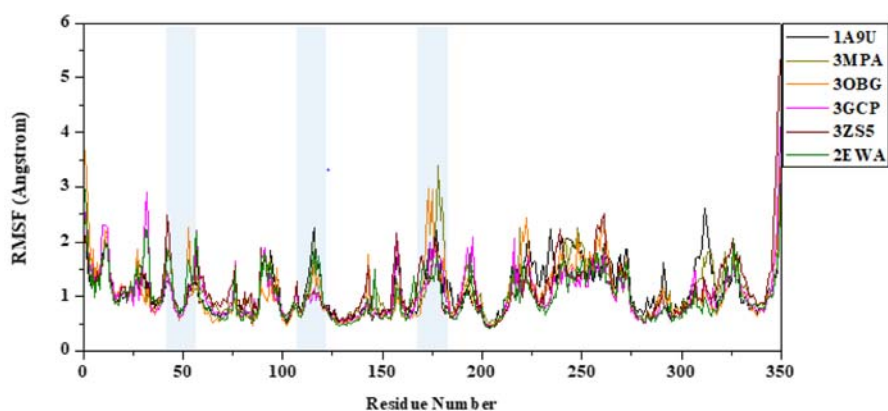


Figure 3. RMSF of each residue of the protein for all six complexes obtained from 10 ns MD simulations.

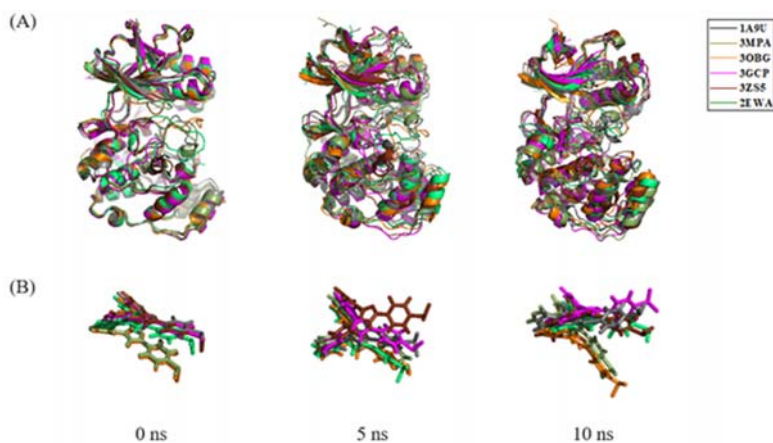


Figure 4. Superimposition of the six MD structures at 0, 5 and 10 ns simulations.

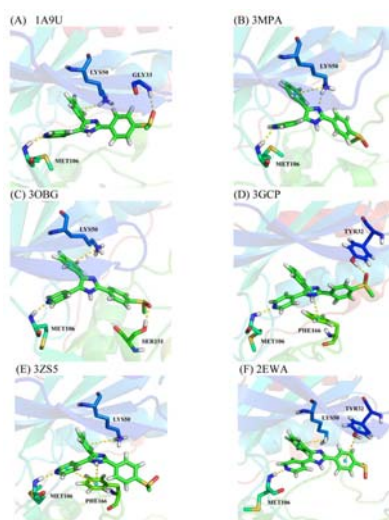


Figure 5. Binding interaction of SB-203580 in the active sites; (A) 1A9U, (B) 3MPA, (C) 3OBG, (D) 3GCP, (E) 3ZS5 and (F) 2EWA. Yellow dots represent hydrogen bond and stacking interactions.

In summary, the hydrogen bond plays an important role in type I inhibitor binding to ATP site of the kinase. The SB-203580 inhibitor forms stable hydrogen bond with Gly33, Lys50, Met106, and Ser151. The inhibitor interacted with Met106 in the hinge region that is a stable hydrogen bond. And the SB-203580 formed pi stacking interactions with Tyr32, Lys50, and Phe166 that are found in the DFG-out conformation. The position of fluorobenzene, imidazole, pyridine, and sulfoxide are important in the SB-203580 structure for interaction with DFG-in and DFG-out of the kinase that is shown in Figure 6.

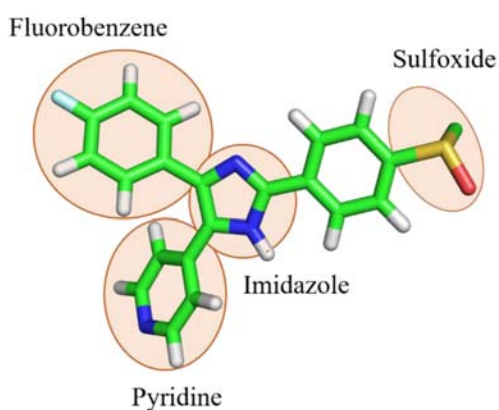


Figure 6. Structure of type I inhibitor of the kinase (SB-203580).

3.3 Conformation of Inhibitor Type II in DFG-out Kinase

MD simulations of DFG-out protein complexes with type II inhibitors (Inhibitors A-D) -p38 MAP kinase are studied. The structures are similar in aryl urea group but the difference is methyl benzyl and chloride group as shown in Figure 7.

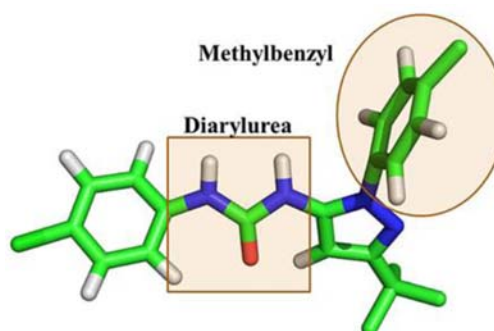
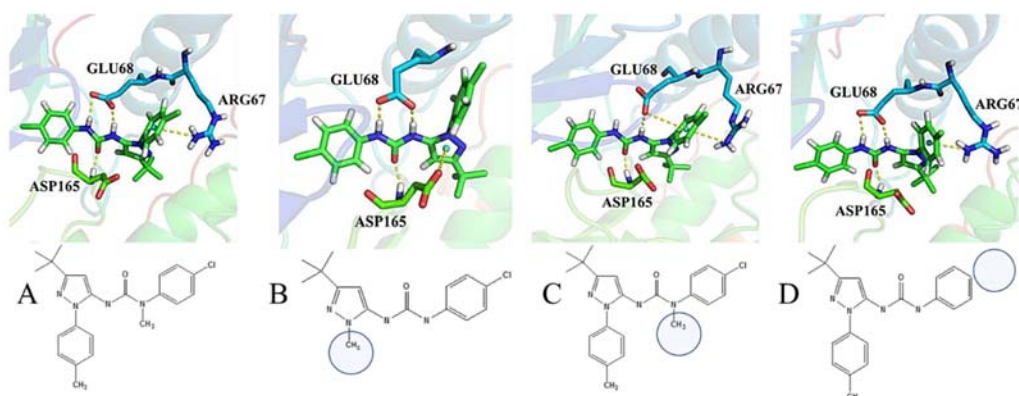


Figure 7. Structure of type II inhibitor, there are aryl urea and methyl benzyl group in the structure.

To describe type II inhibitor -p38 MAK kinase interactions in the binding site based on free energy calculations, Figure 8 shows the interactions of the inhibitors with the amino acids in the active site. It can be seen that the oxygen of Glu68 forms a hydrogen bond with H atom of diaryl urea of inhibitor which are found for all systems. The HN- group of Asp165 forms hydrogen bond with diaryl urea of inhibitor. In the part of methyl benzyl of inhibitor, it forms pi-stacking networks among Arg67. Inhibitor B does not form pi-stacking because of the lack of methyl benzyl group. However, structure B forms pi-stacking at pyrazol group of inhibitors (Figure 8B). The DFG- out conformation of 1KV1 also forms the hydrogen bond at Asp165. The hydrogen bond and pi-stacking also found to play an important role in type II inhibitor binding to allosteric site of the kinase.



A = 1-(5-Tert-Butyl-2-Methyl-Benzyl-2H-Pyrazol-3-yl)-3-(4-Chloro-Phenyl)-4-Methyl-Urea

B = 1-(5-Tert-Butyl-2-Methyl-2H-Pyrazol-3-yl)-3-(4-Chloro-Phenyl)-Urea

C = 1-(5-Tert-Butyl-2-Methyl-Benzyl-2H-Pyrazol-3-yl)-3-(4-Chloro-Phenyl)-Urea

D = 1-(5-Tert-Butyl-2-Methyl-Benzyl-2H-Pyrazol-3-yl)-3-Phenyl-4-Methyl-Urea

Figure 8. Structural representative snapshot of type II inhibitor from MD of with protein 1KV1. Yellow dashed line represents hydrogen bond and stacking interactions.

3.4 Free Energy Calculations of $\Delta\Delta G$

The binding free energies of four systems are calculated by using TI simulations. The relative free energy of binding $\Delta\Delta G$ is determined from the difference in the change in free energy of performing the same free in solution and bound to the protein in water. The results are shown in

Table 2 and Figure 9. The displays calculated $\langle dV/d\lambda \rangle_\lambda$ and its standard deviation at λ points. A straight forward evaluation gives a relative binding free energy of -4.12 kJ/mol, in good agreement with the experimental value of -3.28 kJ/mol, based on values of K_D of 8, 1160, 7500 and 21 nM for inhibitors and its analog, respectively [21, 35].

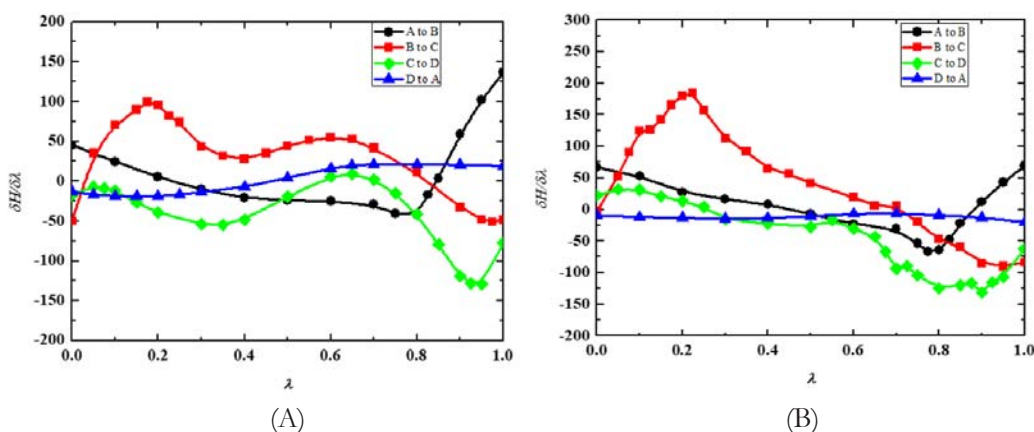


Figure 9. Calculated $\delta H/\delta\lambda$ and its standard deviation at λ points for four type II inhibitors in solution (A) and protein (B) states.

The key features regarding the inhibitor-based contributions to the free energy difference are summarized as follows in Table 2. The small four type II inhibitors contributions in solution are 2.67, 32.35, -38.03, and 2.93 kJ/mol for inhibitor A, B, C and D, respectively that the total of TI free energy was -0.08 kJ/mol. Their contributions

in kinase protein are 7.86, 39.53, -40.01, and -11.50 kJ/mol which the total cycle of TI free energy was -4.12 kJ/mol. From the results, the position of diaryl urea in type II inhibitor structure interacts with Asp165 of DFG-out in kinase by hydrogen bond. The part of methyl benzyl in type II inhibitor interacts with Arg67 and Glu68 by pi-stacking interaction.

Table 2. Calculated free energy changes (kJ/mol).

	ΔG_{exp} (kJ/mol)		ΔG_{exp} (kJ/mol)	ΔG_{prot} (kJ/mol)	ΔG_{solv} (kJ/mol)	$\Delta G_{\text{exp}}^{\text{a}}$ (kJ/mol)	$\Delta G_{\text{prot}} - \Delta G_{\text{exp}}^{\text{a}}$ (kJ/mol)
A	-46.21	A to B	12.33	7.86	2.67	-3.67	11.53
B	-33.88	B to C	4.63	39.53	32.35	37.35	2.18
C	-29.25	C to D	-14.57	-40.01	-38.03	-26.03	-13.98
D	-43.82	D to A	-2.39	-11.50	2.93	-10.93	-0.57
Total			0	-4.12	-0.08	-3.28	-0.84

^a Free energy of inhibitor in water from experiment.

4. CONCLUSION

Significant differences between six structures of P38 MAP kinase and type I inhibitor are restricted to the ATP-binding pocket, where ligand-induced conformational differences are observed in the hinge region (His104 and Met106) and the DFG motif. SB-203580, type I inhibitor is bound mostly in the regions that are conserved in protein kinase for the bonding of ATP. The DFG-out strongly inhibited by SB-203580 that the interaction is the aromatic stacking interaction between the phenyl group of the inhibitor and Tyr32, which point into the ATP pocket. As shown from the MD results, the binding of SB-203580 in the DFG-in and mutant DFG-in proteins revealed more stable binding than that in DFG-out.

Using p38 MAP kinase as a model system for TI free energy, we computed the conformational and binding free energies of the type II inhibitor and p38 MAP kinase using the GROMACS algorithm. Our computational calculations successfully

sampled multiple conformations of DFG-out states, and the conformational fluctuations are exposed of the activation loop in the allosteric binding site, DFG motif. The interactions and the conserved Arg67, Glu68, and Asp165 have a role in stabilizing states between type II inhibitor and kinase protein. However, the structure of inhibitor B in type II inhibitor does not interact with Arg67, and Glu68 because there is not methyl benzyl function in the structure. Therefore, the position of diaryl urea and methyl benzyl are important in the type II inhibitor structure to interact with residues in the allosteric binding pocket of p38 MAP kinase. This result suggests that the type I and II inhibitors are good inhibitors and are interested to develop for future p38 MAP kinase assays.

ACKNOWLEDGEMENTS

This work is partially supported by grants from Kasetsart University, the Center for Advanced Studies in Nanotechnology

and Its Applications in Chemical, Food and Agricultural Industries (a scholarship to WB), The Thailand Research Fund (RTA5380010 and DBG5980001), the Commission on Higher Education, National Electronics and Computer Technology Center and Faculty of Science, Kasetsart University. We thank Dr. Alpesh Kumar K. Mald, and Prof. Alan E. Mark for valuable comments and helping on the TI free energy calculations and facilities.

CONFLICT OF INTEREST

We declare that we have no competing interests.

STATEMENT OF AUTHORSHIP

W. Boonyarat designed, calculations, collected and analyzed the data, W. Boonyarat and P. Saparpakorn discussed and drafted the manuscript. S. Hannongbua designed and conducted the study. All authors read and approved the final manuscript.

REFERENCES

- [1] Bukhtiyarova M., Karpusas M., Northrop K., Namboodiri H.V.M. and Springman E.B., *Biochemistry*, 2007; **46**: 5687-5696. DOI 10.1021/bi0622221.
- [2] Freshney N.W., Rawlinson L., Guesdon F., Jones E., Cowley S., Hsuan J. and Saklatvala J., *Cell*, 1994; **78**: 1039-1049. DOI 10.1016/0092-8674(94)90278-X.
- [3] Han J., Lee J., Bibbs L. and Ulevitch R., *Science*, 1994; **265**: 808-11. DOI 10.1126/science.7914033.
- [4] Han J., Jiang Y., Li Z., Kravchenko V.V. and Ulevitch R.J., *Nature*, 1997; **386**: 296-9. DOI 10.1038/386296a0.
- [5] Lee J.C., Laydon J.T., McDonnell P.C., Gallagher T.F., Kumar S., Green D., McNulty D., Blumenthal M. J., Keys J.R., Land vatter S.W., Strickler J.E., McLaughlin M.M., Siemens I.R., Fisher S.M., Livi G.P., White J.R., Adams J.L. and Young P.R., *Nature*, 1994; **372**: 739-746. DOI 10.1038/372739a0.
- [6] Kumar S., Boehm J. and Lee J.C., *Nat. Rev. Drug Discov.*, 2003; **2**: 717-726. DOI 10.1038/nrd1177.
- [7] Zhang X.H., Nam S., Wu J., Chen C.H., Liu X., Li H., McKeithan T., Gong Q., Chan W.C., Yin H.H., Yuan Y.C., Pillai R., Querfeld C., Horne D., Chen Y. and Rosen S.T., *J. Invest. Dermatol.*, 2018. DOI 10.1016/j.jid.2018.04.030.
- [8] Huse M. and Kuriyan J., *Cell*, 2002; **109**: 275-282. DOI 10.1016/S0092-8674(02)00741-9.
- [9] Sun H., Tian S., Zhou S., Li Y., Li D., Xu L., Shen M., Pan P. and Hou T., *Sci. Rep.*, 2015; **5**: 8457. DOI 10.1038/srep08457.
- [10] Apsel B., Blair J.A., Gonzalez B., Nazif T.M., Feldman M.E., Aizenstein B., Hoffman R., Williams R.L., Shokat K.M. and Knight Z.A., *Nat. Chem. Biol.*, 2008; **4**: 691-699. DOI 10.1038/nchembio.117.
- [11] Schindler T., Bornmann W., Pellicena P., Miller W.T., Clarkson B. and Kuriyan J., *Science*, 2000; **289**: 1938-1942. DOI 10.1126/science.289.5486.1938.
- [12] You W. and Chang C.E.A., *J. Chem. Inf. Model.*, 2018. DOI 10.1021/acs.jcim.7b00640.
- [13] Badrinarayan P. and Sastry G.N., *J. Chem. Inf. Model.*, 2011; **51**: 115-129. DOI 10.1021/ci100340w.
- [14] Atzori A., Bruce N.J., Burusco K.K., Wroblowski B., Bonnet P. and Bryce R.A., *J. Chem. Inf. Model.*, 2014; **54**: 2764-2775. DOI 10.1021/ci5003334.
- [15] Kornev A.P., Haste N.M., Taylor S.S. and Ten Eyck L.F., *Proc. Natl. Acad. Sci.*, 2006; **103**: 17783-17788. DOI 10.1073/pnas.0607656103.

- [16] Janne P.A., Gray N. and Settleman J., *Nat. Rev. Drug Discov.*, 2009; **8**: 709-723. DOI 10.1038/nrd2871.
- [17] Azevedo R., van Zeeland M., Raaijmakers H., Kazemier B., de Vlieg J. and Oubrie A., *Acta Crystallogr. Sect. D*, 2012; **68**: 1041-1050. DOI 10.1107/S090744491201997X.
- [18] Vogtherr M., Saxena K., Hoelder S., Grimme S., Betz M., Schieborr U., Pescatore B., Robin M., Delarbre L., Langer T., Wendt K.U. and Schwalbe H., *Angew. Chem. Int. Ed.*, 2006; **45**: 993-997. DOI 10.1002/anie.200502770.
- [19] Regan J., Breitfelder S., Cirillo P., Gilmore T., Graham A.G., Hickey E., Klaus B., Madwed J., Moriak M., Moss N., Pargellis C., Pav S. Proto A., Swiname A., Tong L. and Torcellini C., *J. Med. Chem.*, 2002; **45**: 2994-3008. DOI 10.1021/jm020057r.
- [20] Van Der Spoel D., Lindahl E., Hess B., Groenhof G., Mark A.E. and Berendsen H.J.C., *J. Comput. Chem.*, 2005; **26**: 1701-1718. DOI 10.1002/jcc.20291.
- [21] Schmid N., Eichenberger A., Choutko A., Riniker S., Winger M., Mark A. and van Gunsteren W., *Eur. Biophys. J.*, 2011; **40**: 843-856. DOI 10.1007/s00249-011-0700-9.
- [22] Wilson K.P., McCaffrey P.G., Hsiao K., Pazhanisamy S., Galullo V., Bemis G.W., Fitzgibbon M.J., Caron P.R., Murcko M.A. and Su M.S.S., *Chem. Biol.*, 1997; **4**: 423-431. DOI 10.1016/S1074-5521(97)90194-0.
- [23] Simard J.R., Getlik M., Grutter C., Pawar V., Wulfert S., Rabiller M. and Rauh D., *J. Am. Chem. Soc.*, 2009; **131**: 13286-13296. DOI 10.1021/ja902010p.
- [24] Malde A.K., Zuo L., Breeze M., Stroet M., Poger D., Nair P.C., Oostenbrink C. and Mark A.E., *J. Chem. Theory Comput.*, 2011; **7**: 4026-4037. DOI 10.1021/ct200196m.
- [25] Berendsen H.J.C., Postma J.P.M., van Gunsteren W.F. and Hermans J., *Intermol. Forces*, 1981; 331-342. DOI 10.1007/978-94-015-7658-1_21.
- [26] Berendsen H.J.C., Postma J.P.M., van Gunsteren W.F., DiNola A. and Haak J.R., *J. Chem. Phys.*, 1984; **81**: 3684-3690. DOI 10.1063/1.448118.
- [27] Ryckaert J.P., Ciccotti G. and Berendsen H.J.C., *J. Comput. Phys.*, 1977; **23**: 327-341. DOI 10.1016/0021-9991(77)90098-5.
- [28] van Gunsteren W.F., Beutler T.C., Fraternali F., King P.M., Mark A.E. and Smith P.E., *ESCOM Sci. Publ. Leiden*, 1989. DOI 10.1007/978-94-017-1120-3.
- [29] Beutler T.C., Mark A.E., van Schaik R.C., Gerber P.R. and van Gunsteren W.F., *Chem. Phys. Lett.*, 1994; **222**: 529-539. DOI 10.1016/0009-2614(94)00397-1.
- [30] Zacharias M., Straatsma T.P. and McCammon J.A., *J. Chem. Phys.*, 1994; **100**: 9025-9031. DOI 10.1063/1.466707.
- [31] Allen M.P. and Tildesley D.J., *Oxford Univ. Press Inc.*, New York. 1989.
- [32] Horjales S., Schmidt-Arras D., Limardo Ramiro R., Leclercq O., Obal G., Prina E., Turjanski A.G., Spath G.F. and Buschiazzo A., *Structure*, 2012; **20**: 1649-1660. DOI 10.1016/j.str.2012.07.005.
- [33] Hari Sanjay B., Merritt Ethan A. and Maly Dustin J., *Chem. Biol.*, 2014; **21**: 628-635. DOI 10.1016/j.chembiol.2014.02.016.
- [34] Huang Y.mingM., Chen W., Potter Michael J. and Chang C.enA., *Biophys. J.*, 2012; **103**: 342-351. DOI 10.1016/j.bpj.2012.05.046.
- [35] Simard J.R., Grutter C., Pawar V., Aust B., Wolf A., Rabiller M. and Rauh D., *J. Am. Chem. Soc.*, 2009; **131**: 18478-88. DOI 10.1021/ja907795q.